Hindawi
Journal of Nanomaterials
Volume 2022, Article ID 7583032, 9 pages
https://doi.org/10.1155/2022/7583032

Research Article

Nanoconjugation between Fungal Nanochitosan and Biosynthesized Selenium Nanoparticles with *Hibiscus sabdariffa* Extract for Effectual Control of Multidrug-Resistant Bacteria

Mohammed S. Al-Saggaf

College of Science and Humanitarian Studies, Shaqra University, Al Quwaiiyah 11971, Saudi Arabia

Correspondence should be addressed to Mohammed S. Al-Saggaf; dr.alsaggaf10@gmail.com

Received 31 December 2021; Accepted 10 March 2022; Published 21 March 2022

Academic Editor: Thathan Premkumar

Multidrug-resistant (MDR) pathogenic bacteria are hazardous and ongoing threats worldwide, which urges searching for novel bioeffectual alternatives for combating MDR attacks. Herein, it was targeted to extract chitosan (Cht) from fungal culture (*Mucor circinelloides*) and transform it to nanochitosan (NCht), to biosynthesize selenium nanoparticles (SeNPs) directly using *Hibiscus sabdariffa* extract (HbE), and to conjugate these bioactive agents and assess their biocidal actions against MDR bacterial pathogens (*Klebsiella pneumoniae*, *Salmonella typhimurium*, and *Staphylococcus aureus*). The fungal Cht had 86.71% deacetylation and transformed effectually to NCht with a 67.6 nm average particle diameter. The SeNPs were innovatively and simply biosynthesized by direct interaction with HbE, which were validated visually, calorimetrically, and biochemically; the HbE/SeNPs had a 12.1 nm mean size. The conjugation between NCht and HbE/SeNPs was proven via structural and biochemical analysis. The entire fabricated NPs/nanocomposites exhibited elevated bactericidal actions toward all MDR pathogens; NCht/HbE/SeNPs were the most powerful with the widest growth inhibition zones and minimal bactericidal concentrations. The most sensitive bacteria were *K. pneumoniae*, whereas *S. aureus* displayed the utmost resistance. The ultrastructure of treated *K. pneumoniae* with NCht/HbE/SeNPs evidenced the attachment of nanocomposite particles to bacterial membranes and the full bacterial lysis/death within 8 h of exposure. The compositing of NCht with HbE-biosynthesized SeNPs provided powerful ideal bactericidal conjugates against MDR pathogens with warranted biosafety, eco-friendliness, and effectuality.

1. Introduction

Nanotechnology includes interdisciplinary branches of research that have attracted excessive global attention due to their direct impacts on human life; the nanotechnological methods should preferably have environment-friendly, economical, and feasible attributes, which could be warranted all from the biological synthesis approaches, compared to chemical and physical methods of synthesis [1].

The nanoparticles (NPs) of metals were extensively employed in diverse biomedical sectors, e.g., antioxidant, antibacterial, anticoagulant, and anticancer, due to their extraordinary functionality and reactivity [2]. Amid biosynthesized metal NPs, selenium NPs (SeNPs) appealed extensive consideration for their exceptional physicochemical physiognomies, which include NP biocompatibility, reduced toxicity, chemical stability, and bioactivity [3, 4]. Se is the crucial trace mineral for maintaining human functions and health, with daily requirements of ~40–300 mg for adults; the Se deficiency could associate with >40 human diseases [5]. The human body can naturally assimilate/degrade Se and SeNPs; the SeNP leftovers can serve as a supplementary nutritional source for Se, which are nontoxic to humans within the required limits [6, 7]. The main bioactivities of SeNPs included their employment in antibacterial formulation, cancer treatment, and drug delivery [5].

Infectious disease mortality/morbidity consists of a prominent percentage of human death worldwide. The main health-observing agencies continually expressed the serious threats of

multidrug resistance (MDR) emergence in bacterial pathogens, which could resist the antimicrobial actions of most accustomed antibiotics [8]. Originally, MDR bacteria were restricted within hospitals and intensive care units, but nowadays, they were detected and attacked everywhere [9]. These issues urged searches for initiatives to develop innovative antimicrobial agents/composites with more deliverability, safety, and biocidal effectuality to combat such MDR pathogens. The main reported MDR species include various strains of Gram-positives (e.g., *Enterococcus* spp., *Staphylococcus* spp., and *Streptococcus* spp.) and Gram-negatives (e.g., *Acinetobacter* spp., *Escherichia coli*, *Pseudomonas* spp., *Klebsiella* spp., and *Salmonella* spp.) [8, 9]. Diverse approaches/materials were employed for MDR pathogen control, including synthesizing, assessing, and applying phytocompounds, biopolymers, and nanostructured materials [10, 11]. Nanomaterials, including nanometals and nanopolymers, possessed potent antimicrobial actions, either individually or as carriers for further bioactive molecules to enable their delivery into microbial cells and synergize their actions [8, 12]. Further approaches involved the incorporation of combined plant-based and biopolymer antimicrobials with metal nanoparticles to minimize their biotoxicity issues; these strategies were effectual for inhibiting numerous microbial pathogens, including MDR cells [8, 11, 12].

Hibiscus sabdariffa (Roselle) are cultivated plants in numerous subtropical/tropical countries in Asia and Africa; these plants are greatly usable in herbal tea due to their fruitful water-soluble contents from anthocyanin compounds, flavonoids, hibiscus acids, and ascorbic acid [13]. The *H. sabdariffa* extract (HbE) could be promisingly used for nanometal green synthesis, mainly because of its contents from antioxidant and reducing anthocyanins [14]. HbE was earlier employed for diverse nanometal biosynthesis (including CeO_2, Au, CdO, ZnO, and graphene oxide NPs) [13, 14]. However, no reports are obtainable regarding the usage of HbE for selenium NP synthesis and their application as antimicrobial agents against MDR bacteria.

Chitosan (Cht), the derived biopolymer from deacetylated chitin, has numerous precious characteristics/applications in human care (including usage in nutritional, biomedical, healthcare, environmental, pharmaceutical, and biotechnological fields) [15]. Cht possesses very auspicious antimicrobial potentialities toward frequent genera; promisingly, the Cht biosafety was verified toward animals and humans [16–19]. The conjugation of Cht with further bioactive agents/compounds (e.g., plant extracts, phytocompounds, metal NPs) was stated to augment their combined microbicidal actions [20–24]. The utilization of fungal biomasses as raw material for Cht extraction, as alternatives to traditional sources from crustacean shells, emerged recently to provide sustainable, controllable, and cost-effective sources for this precious product, employing different species of fungal cultures [15, 16, 18, 21, 25–27]; they reported comparable or even higher bioactivities of fungal Cht than the products from accustomed sources.

Cht nanoparticles (NCht), especially from fungal origins, have attracted much interest due to astonishing biochemical attributes (e.g., elevated biocompatibility, biodegradability, minimum toxicity, drug/biomolecule-carrying ability, antimicrobial powers, anticancer action, and synergism with bioactive molecules) [22, 27, 28].

The NCht was effectually used for carrying diverse biomolecules and nanometals to augment their biosafety, deliverability to target cells, antimicrobial, antioxidant, and anticancerous capabilities [19, 28–30].

Accordingly, it was targeted here to extract Cht from fungal culture (*Mucor circinelloides*) and transform it to NCht, to biosynthesize SeNPs directly using HbE, and to conjugate these bioactive agents and assess their biocidal actions against MDR bacterial pathogens.

2. Materials and Methods

2.1. Fungal Chitosan (Cht) Extraction. Fungal culture, *Mucor circinelloides* (DSM-1191), was employed herein for Cht production [16], after growing and maintaining fungi using potato dextrose media (broth and agar; Oxoid, Basingstoke, UK) at 28°C for 8 days, aerobically. The Cht extraction began by harvesting fungal mycelia via filtration, washing with deionized water (DW), and drying with an air oven at 45 ± 2°C for 30 h. The transformation of dried mycelia to Cht involved (1) deproteinization (via soaking in 20 folds, *w*/*v*, of 1.0 M of NaOH for 8 h without heating); (2) demineralization (via soaking in 20 folds, *w*/*v*, of 1.0 M acetic acid for 6 h without heating); and (3) deacetylation (with 30 folds, *w*/*v*, of 56% NaOH solution for 88 min at 112°C). Filtration, DW washing, and air-drying were performed for fungal materials after each former step. The Cht deacetylation degree (DA %) was calculated from its spectrum absorbance in FTIR (Fourier-transform infrared spectroscopy), using the next formula: $\mathrm{DA}\,(\%) = 100 - (\mathrm{A}\ 1655/\mathrm{A}\ 3450 \times 115)$.

2.2. Synthesis of Nanofungal Chitosan (NCht). NCht synthesis from produced Cht depended on former methods [19, 22], using the ionic gelation technique. After Cht solution preparation (0.1% (*w*/*v*) in acetic acid aqueous solution (1.5%, *v*/*v*)) and Na-TPP (sodium tripolyphosphate) solution (0.1%, *w*/*v*, in DW), the solution of Na-TPP was deliberately dropped (with 350 μL/min rate) into speedily stirred Cht solution, until reaching a ratio of 3 : 1 (*w*/*w*) from Cht : Na-TPP. The stirring was sustained for 75 min following Na-TPP dropping, and the illuminated NCht-containing suspension was centrifuged (25000 × *g* for 25 min), DW washed, recentrifuged, frozen, and lyophilized.

2.3. Hibiscus Extract (HbE) Preparation. Dry identified Roselle or hibiscus calyces (*Hibiscus sabdariffa*) were acquired from the SNH-KSU (Saudi National Herbarium-King Saud University, Riyadh, KSA). Powdered and sieved calyx powders (~50 mesh) were soaked into 12-folds (*w*/*v*) of 70% ethanol and kept for 25 h under rotation (170 × *g* at 25 ± 2°C). After discarding plant residues via filtration, the resulting hibiscus extract (HbE) was dried via vacuum evaporation at 42°C and kept in the dark.

2.4. Biosynthesis of SeNPs and Their Composites. The SeNP phytosynthesis using HbE involved the preparation of sodium selenite solution (10 mM, Na_2SeO_3; Sigma-Aldrich)

and its combination with HbE aqueous solution (equal volumes) to have an ending HbE concentration of 1.0% (*w*/*v*). The applied conditions for NP biosynthesis were the dark stirring at 220 × *g* and 25 ± 2°C for 300 min. The transformed solution color into deep orange was the visual indicator for SeNP synthesis. The HbE-phytosynthesized SeNPs (HbE/SeNPs) were harvested by centrifuging at 11800 × *g* at 12°C for 32 min (Sigma 2-16P-10350 centrifuge; GmbH, Germany), washed with DW for 3 cycles, recentrifuged, and analyzed for characterization [4].

For compositing of nanoconjugates, from HbE/SeNPs and NCht, stock solutions from both agents (0.1%, *w*/*v*) were prepared in DW and 1% acetic acid, respectively, vigorously stirred, and sonicated for 5 min. From NP solutions, equal volumes were intermingled and under stirring (680 × *g*) for 85 min, and then formed NP conjugates (NCht/HbE/SeNPs) were acquired through centrifugation, DW washed, recentrifuged, frozen, and then lyophilized.

2.5. Analysis of NP/Nanoconjugate Physiognomies

2.5.1. FTIR Spectral Analysis. The spectroscopic infrared spectra of HbE, NCht, HbE/SeNPs, and their combined conjugates were assessed from FTIR transmission mode (Fourier-transform infrared spectroscopy, PerkinElmer, Germany), after samples were amalgamated with 1.0% KBr.

2.5.2. Nanoparticle Size (Ps) and Charges. The DLS (dynamic light scattering technique) was used for appraising Ps distribution and the zeta (ζ) potentials of fabricated NCht, HbE/SeNPs, and NCht/HbE/SeNPs, using Nano ZS Zetasizer (Malvern, Southborough, MA).

2.5.3. Structural Analysis. The ultrastructure imaging of HbE-synthesized SeNPs was screened via TEM (transmission electron microscopy, JEOL JEM-2200FS, Japan) to assess their size, morphology, shape, and distribution.

2.6. Antimicrobial Assessment against Multidrug-Resistant (MDR) Bacteria

2.6.1. In Vitro Antimicrobial Assessment. Standard MDR bacterial strains, i.e., *Klebsiella pneumoniae* subsp. pneumoniae (ATCC 51504; multidrug-resistant), *Staphylococcus aureus* (ATCC 43300; oxacillin/methicillin-resistant), and *Salmonella typhimurium* (*Salmonella enterica* subsp. enterica serovar Typhimurium; ATCC BAA-190; multidrug-resistant), were grown and challenged in nutrient broth and agar media (NB and NA, respectively), aerobically at 37 ± 1°C. The antibacterial capabilities of fabricated NPs/nanoconjugates were valued using IZ assay (growth inhibition zones around assay discs) and MBC determination (minimal bactericidal concentration, μg/mL).

In IZ assay, bacterial cell suspensions in NB were swabbed homogenously onto the NA surface, and then filter paper sterilized discs (Whatman No. 2, 6 mm diameter) impregnated with NP/nanoconjugate solutions (25 μL/disc, from 50 μg/mL concentration) were situated over the inoculant and incubated for 18–26 h aerobically at 37 ± 1°C. The diameters of appeared IZs were measured precisely in triplicate. The examined bacterial strains were also assessed for their sensitivity toward standard antibiotic discs, i.e., amoxicillin/clavulanic acid, ceftazidime, ciprofloxacin, chloramphenicol, doxycycline, gentamicin, levofloxacin, and norfloxacin (Fluka, Switzerland), which are considered positives controla, while the discs impregnated with DW and 1% acetic solution served as negatives controls.

The MBCs of NPs/nanoconjugates were determined with the microdilution technique, which was confirmed via triphenyl tetrazolium chloride indicator staining, at a nanocomposite concentration of the 1.0–50.0 μg/mL range [31].

2.6.2. SEM (Scanning Electron Microscopy) Imaging. The antibacterial action mechanism of NCht/HbE/SeNPs against MDR *K. pneumoniae*, as a pathogen model, was screened via SEM imaging (JEOL JSM-IT100, Japan), after exposure and incubation with nanoconjugates (15 μg/mL concentration) for 4 and 8 h. The capturing indicated the alterations/distortions in the exposed cell morphology and structure.

2.7. Statistical Analysis. Experimental trial (triplicate) results were analyzed statistically using the SPSS package (V 11.5; Chicago, IL), for appraising the significant differences at $p \leq 0.05$.

3. Results and Discussion

3.1. Fungal Cht Production. The fungal Cht was efficaciously extracted from *M. circinelloides* biomass with a yield of 38.42 mg/g of dry biomass. The produced fungal Cht had a DD of 86.71%, a creamy color, and 97.42% solubility in 1% acetic acid solution without heating. The attained results agree with former investigations that involved Cht production from further fungal species, including *Agaricus* spp., *Aspergillus* spp., *Mucor* spp., *Absidia* spp., and *Cunninghamella* spp. [15, 18, 27].

3.2. FTIR Analysis of Produced Molecules. The FTIR spectral investigations were performed to identify potential biomolecules in generated agents (NCht, HbE, HbE/SeNPs, and their composites) and their interactions and roles in NP synthesis/stabilization (Figure 1).

The main distinctive bands in NCht were parallel to their original bands in native fungal chitosan; this was recurrently evidenced from the former works in fungal NCht [22, 26, 28, 29]. The appeared distinctive bands in the NCht spectrum appointed and confirmed its correlation and origin from fungal Cht, as shown in Figure 1 (NCht). These bands included the sharp band at 2893 cm^{-1} (indicating the C–H bond stretched vibrations), the band at 1722 cm^{-1} (appointed the C=O group stretched vibrations), and the band at 1440 cm^{-1} (appointed the hydroxyl group (O–H)) [27, 29]. The intense band at 1098 cm^{-1} corresponds to –C–O–C– group stretched vibrations, which are characteristics for biopolysaccharides [28], whereas the 846 cm^{-1} band indicated the NCht amine groups [31].

The FTIR pattern of HbE (Figure 1, HbE) displayed many peaks within the 1108 and 1072 cm^{-1} range, indicating the existence of anthocyanin types in HbE (e.g., delphinidin-3-*O*-sambubioside and cyanidin-3-*O*-sambubioside) [32].

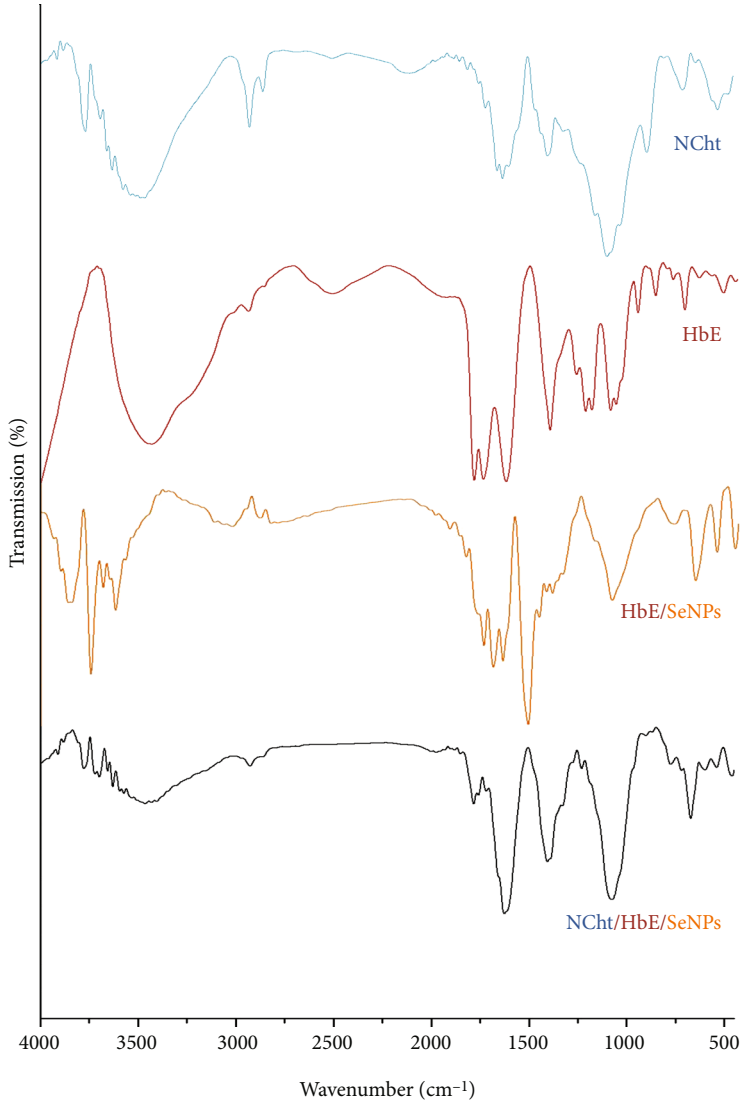

Figure 1: FTIR spectra of nanochitosan (NCht), hibiscus extract (HbE), synthesized SeNPs with HbE (HbE/SeNPs), and their composites (NCht/HbE/SeNPs).

The perceived peak at ~1259 cm^{-1} is ascribed to the O–C stretching of acid groups [33]. The wide peak at 3423 cm^{-1} is biochemically attributed to O–H vibrated stretching, whereas the apparent peak at ~1784 cm^{-1} is associated with C=O stretching, and the C=N pull is assigned from the peak at ~1616 cm^{-1} [34]. The angular deformation vibrations of CH_3 and N–H were evidenced from peaks at ~1368 cm^{-1} and~768 cm^{-1}, respectively [33, 34], whereas the observed strong peak at 1223 cm^{-1} indicates the alkyl vinyl ether asymmetric stretching [27].

The interactions between HbE and SeNPs were evidenced from the FTIR spectrum of their conjugates (Figure 1, HbE/SeNPs). The wide band at 3423 cm^{-1} in the HbE spectrum (O–H vibrated stretching) mostly disappeared in the HbE/SeNP spectrum, indicating the key role of this group/bond in SeNP reduction. Additionally, the indicating band of anthocyanins at 1072 cm^{-1} disappeared in the nanoconjugate spectrum, as well as the designative band of alkyl ethers at 1223 cm^{-1}. Many characteristic bands emerged in the HbE/SeNP spectrum, which could not be detected in the original HbE spectrum (e.g., at 1506, at 1897, and in the range of 3610-3860 cm^{-1}), which strongly indicates the potential new interactions between HbE biomolecules and SeNPs during their biosynthesis.

HbE has strong antioxidant potentialities (mainly attributed to anthocyanin contents) that could induce metal reduction from their precursor salts; the anthocyanin moieties' stabilized NPs are the detected products, which is confirmed via FTIR analysis [27]. Additionally, the HbE reducing and stabilizing activities were proved for the synthesis of AgNPs, and these activities were attributed to HbE active phytoconstituents such as acids, anthocyanins, and phenolic compounds [35].

The wide band of the O–H (and N–H) stretching around 2450 cm^{-1} in NCht became almost undetectable after conjugation with the extract and nanometals; this could be because such groups can form bonds with further functional groups and, accordingly, cross-linked polymer networks are formed [24, 30].

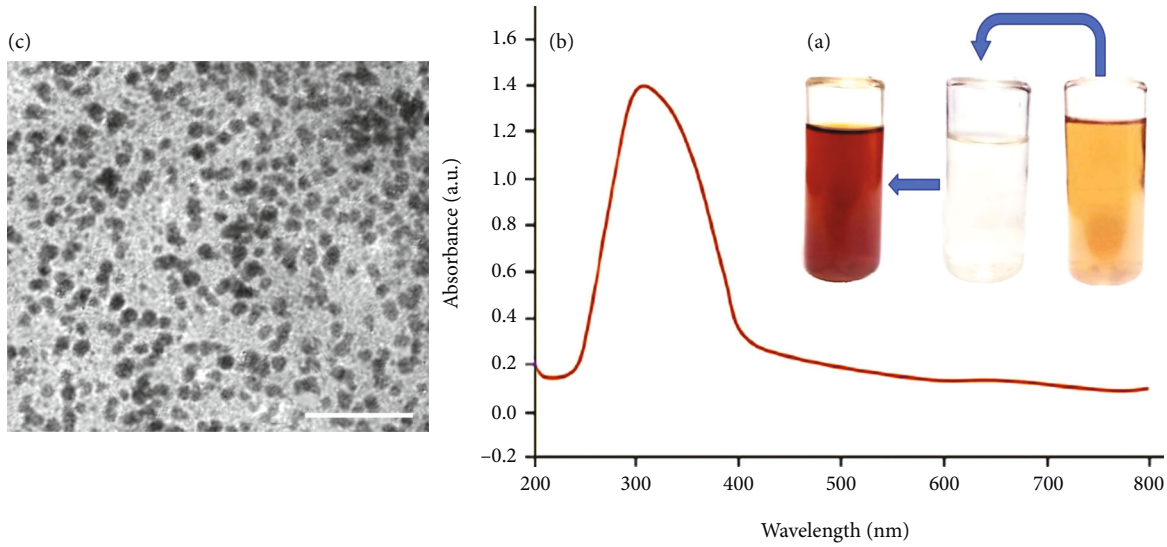

Figure 2: Physiognomic characteristics of biosynthesized SeNPs using hibiscus extract, including their visual appearance (a), UV spectrum (b), and TEM image of NP ultrastructure (c).

Table 1: The Ps distribution and ζ potential of synthesized HbE/SeNPs, NCht, and their nanocomposites.

NPs	Size range (nm)	Mean diameter (nm)	Zeta potential (mV)
HbE/SeNPs	4.7–28.3	12.1	-24.8
NCht	24.8–106.6	67.6	+38.7
NCht/HbE/SeNPs	31.4–114.9	73.9	+31.1

3.3. Optical Characterization of Nanoparticles. The visualization of biosynthesized SeNP physiognomic features confirmed the effectiveness of HbE to reduce/stabilize metal NPs (Figure 2). The visual appearance (Figure 2(a)) of NP solution could easily confirm the appearance of the distinctive brownish-orange color of SeNPs after interaction and reduction with HbE. The UV spectrum of HbE-synthesized SeNPs showed a clear distinctive peak at 328 nm (Figure 2(b)), which is in accordance with reported SeNP spectra in former investigations [30, 36]. The NP reduction mechanism is correlated with their SPR (Surface Plasmon Resonance); the excitation of such SPR for specific metal NPs is responsible for their color change and absorbance λ max, which are strong pieces of evidence of NP formation [7, 37].

The TEM imaging of HbE-phytosynthesized SeNPs confirmed their homogenous, uniformed distribution and their effectual stabilization with HbE throughout phytosynthesis (Figure 2(c)); the SeNPs were emphasized with spherical shapes and minimal aggregation. Slight HbE particles were detected within distributed SeNPs, which was formerly appointed for other phytosynthesized SeNPs [31]. The TEM analysis indicated the average SeNP size of 12.32 nm, which agreed with former phytosynthesized SeNP sizes [3, 30, 38], which ranged from 3 to 170 nm, indicating the high effectuality of HbE to reduce/synthesize SeNPs. The elevated contents of bioactive phytoconstituents in HbE (e.g., phenolics, flavonoids, and acids) are assumingly responsible for its high capability for reducing and capping SeNPs [1, 35]; the biomolecules and biocompounds found in plant extracts (e.g., HbE) were verified for NP reduction, stabilization, and aggregation prevention [4, 7].

3.4. NP Charges and Ps Distribution. The ζ potentials and Ps distribution of synthesized nanomaterials/nanocomposites (i.e., HbE/SeNPs, NCht, and NCht/HbE/SeNPs) are indicated using Zetasizer (Table 1). The effectiveness of HbE to promote SeNP synthesis with miniature Ps diameters was verified, with a 12.1 nm mean diameter, which agrees with the average Ps mean obtained from TEM analysis. The NCht had a mean Ps of 67.6 nm, which increased after conjugation with HbE/SeNPs to become 73.9; this indicates the NCht effectiveness for NP capping [19, 30]. While NCht carried strong positive charges (ζ potential = +38.7 mV), the SeNPs were negatively charged (ζ potential = −24.8 mV). The nanoconjugates from the entire agents (NCht/HbE/SeNPs) were positively charged (ζ potential = +31.1 mV), and this indicates the NCht capping of NPs rather than its biochemical interaction with them [39]. The recorded DLS results and ζ potential of inspected NPs signified their elevated stability and dispersity potentialities in solutions [40]. The attained promising findings here, regarding the minute Ps of NCht/HbE/SeNPs and their high stability, are in accordance with former relevant studies using other types of chitosan and phytosynthesis promoters [39, 41].

3.5. Antibacterial Assessment. The bactericidal actions of generated biomolecules/nanoconjugates were assessed qualitatively and quantitatively (e.g., via IZ and MBC, respectively) toward

Table 2: The antibacterial potentials of generated biomolecules and their composites against drug-resistant pathogens.

Examined agents/composites*	Antibacterial potentials**					
	Klebsiella pneumoniae		*Salmonella typhimurium*		*Staphylococcus aureus*	
	IZ*** (mm)	MBC (μg/mL)	IZ (mm)	MBC (μg/mL)	IZ (mm)	MBC (μg/mL)
HbE	12.6 ± 1.1^{a}	37.5	10.6 ± 0.8^{a}	32.5	10.3 ± 0.6^{a}	37.5
HbE/SeNPs	16.8 ± 1.7^{b}	25.0	16.1 ± 1.3^{b}	27.5	15.4 ± 1.2^{b}	30.0
NCht	12.4 ± 1.3^{a}	32.5	11.6 ± 1.0^{a}	30.0	10.8 ± 0.8^{a}	35.0
NCht/HbE/SeNPs	23.5 ± 2.1^{c}	12.5	21.7 ± 1.9^{c}	17.5	19.2 ± 1.3^{c}	22.5

*The screened biomolecules included hibiscus extract (HbE), biosynthesized selenium nanoparticles with HbE (HbE/SeNPs), nanofungal chitosan (NCht), and their combined conjugates (NCht/HbE/SeNPs). **The antibacterial assays included minimal bactericidal concentration (MBC; in the 1-50 μg/mL range) and inhibition zone measurements (IZ, in mm). ***Dissimilar superscript letters in one column indicate significant difference at $p \leq 0.05$.

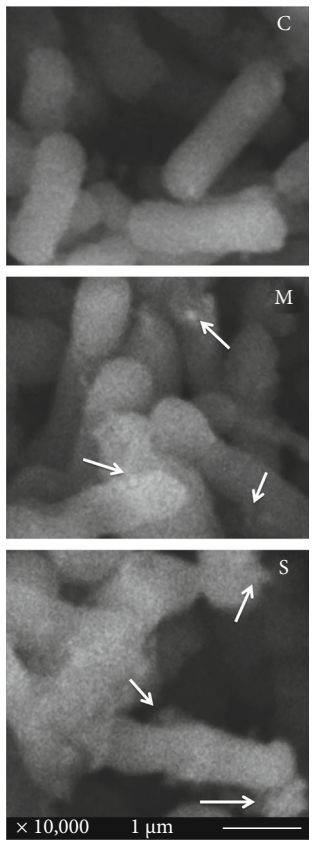

Figure 3: Scanning imaging of treated *Klebsiella pneumoniae* with a nanocomposite of hibiscus extract-synthesized SeNPs and nanofungal chitosan for 4 h (M) and 8 h (S), compared with untreated control (C) cells.

MDR bacterial pathogens (*K. pneumoniae*, *S. typhimurium*, and *S. aureus*) and confirmed via SEM imaging of challenged *K. pneumoniae* cells. The *in vitro* antibacterial assay results indicated the forceful actions of examined agents (HbE, NCht, HbE/SeNPs, and NCht/HbE/SeNPs) against MDR pathogens (Table 2). The entire agents/composites exhibited potent microbicidal actions; the NCht/HbE/SeNP conjugate was significantly the most forceful toward all bacterial strains followed by the HbE/SeNP nanocomposite. The Gram-negative strains (*K. pneumoniae* and *S. typhimurium*) were comparably more sensitive than the Gram-positive strain (*S. aureus*) to examined agents/composites, as evidenced from their IZ diameter and MBC levels. The bacterial strains displayed high resistance to accustomed antibiotics, e.g., amoxicillin/clavulanic acid, ceftazidime, ciprofloxacin, chloramphenicol, doxycycline, gentamicin, levofloxacin, and norfloxacin (data are not presented), using IZ qualitative assay. *K. pneumoniae* was relatively the most sensitive challenged strain, so it was subjected to SEM imaging after exposure to NCht/HbE/SeNPs, to elucidate the potential action modes of the nanocomposite.

3.6. Antibacterial Action Modes via SEM Imaging. The SEM imaging of exposed *K. pneumoniae* to NCht/HbE/SeNPs (Figure 3) displayed that control cells (zero time) appeared with normal, healthy, contacted, and smooth physiognomies (Figure 3, C). After 4 h of exposure to nanoconjugates, apparent deformation and distortion signs could be noticed in cell surfaces; the NPs attached to the cells, which enlarged, partially engorged, and combined with each other (Figure 3, M). The destructive actions of nanoconjugates on exposed cells were observable after 8 h of exposure (Figure 3, S); the cell walls were mostly lysed and deformed, and many NPs and polymer particles appeared in attachment to cells, combined with intracellular released contents. The cells in such a stage completely lost their distinctive exterior and endurance.

The resistance of microbial cells to specific antibiotics depends on the existence/acquisition of resistant gene(s) associated with this antibiotic [10]. However, the MDR microbial pathogen cannot generate resistance to multiple combined antimicrobial compounds with diverse action modes [19, 42], which can clarify the effectuality of examined biomolecules/composites here to inhibit screened MDR bacterial pathogens.

The HbE antibacterial powers were documented by several reports [43–45]; the calyx extracts were also proposed as effectual alternatives for controlling pathogens having multidrug resistance in animals and humans [42]. The high anthocyanin types and polyphenol contents in HbE (e.g., cyanidin-3-sambubioside, delphinidin-3-sambubioside, cyanidin-3-glucoside, and delphinidin-3-glucoside) were suggested to provide substantial antimicrobial, antioxidant, and anti-inflammatory actions in biological systems [43, 45, 46]. Additionally, the HbE antimicrobial action (*in vitro*) was ascribed to its flavonoid contents, which establish strong complexes with microbial cell walls, intensify their permeability, and lead to more penetration of extract and biocidal compounds into the cell

[45]. The HbE mechanisms for the cell permeability increase may include diverse metabolic steps, e.g., suppressing the translocation of electron transport proteins and inhibiting many enzyme-dependent reactions and phosphorylation steps, which enforced membrane swelling and the leakage of intracellular constituents [43].

The microbicidal actions of biogenic synthesized SeNPs were documented and confirmed in numerous investigations against wide varieties of microbial species; they exhibited varied potentialities, but the action was mostly confirmed [5, 6]. The variations in biosynthesized SeNPs' bactericidal activities from diverse plants were supposedly ascribed to the synergistic actions from reducing biogenic phytoconstituents with the actions of SeNPs [31]. The outstanding biocidal mechanisms of SeNPs, for inhibiting cell colonization, growth, and biofilm formation, were mainly attributed to NPs' high oxidative stress and ROS (reactive oxygen species) generation [47]. The Ps impact of SeNPs on their bactericidal potentialities was also demonstrated [48]; the NP biocidal properties were revealed to be size-dependent (as smaller Ps of NPs in the ≤50–100 nm range were more powerful than larger Ps of ≥200 nm). Therefore, the enormously minute Ps of HbE-synthesized SeNPs and the synergistic actions with HbE phytochemicals could provide potential explanations for the forceful antibacterial acts of this nanocomposite [19, 31].

The fungal Cht and NCht were proved to possess remarkable microbicidal actions toward many pathogenic species, including bacterial and fungal strains [16–18, 49]; the main influential factors of this biopolymer are its high surface positivity and free reactive groups, which enable it to interact with microbial cell surfaces and interior constituents, leading to microbial inactivation, lysis, and death. The incorporations of fungal Cht with further biocidal compounds (e.g., metal NPs and plant extracts) were documented to augment their combined microbicidal actions through the synergism between multiple antimicrobial actions from these molecules [20, 21, 25, 26].

The antimicrobial synergism between Cht and SeNPs was additionally stated and demonstrated to provide extra biocidal powers to the composite based on the diverse actions from each agent that could inhibit microbial viability and bioactivities [23, 50].

Furthermore, the conjugation of HbE with Cht polymeric systems strongly enhanced the blend antimicrobial action and was recommended for practical applications against microbial infections [51].

4. Conclusion

The fungal Cht from *M. circinelloides* was achieved and transformed to NCht. The HbE reducing activity was evidenced via SeNP biosynthesis, with favorable physiochemical attributes. The conjugation of NCht with HbE/SeNPs generated a powerful antibacterial composite that was capable of obstructing MDR bacterial pathogens. The nanoconjugate could be effectually employed for the protection and treatment of MDR bacterial infections using biosafe, eco-friendly, and natural biocidal components.

Data Availability

The datasets generated and/or analyzed during the current study are available from the corresponding author on reasonable request.

Conflicts of Interest

The author declares that they have no conflicts of interest.

References

[1] A. Alshehri, M. A. Malik, Z. Khan, S. A. Al-Thabaiti, and N. Hasan, "Biofabrication of Fe nanoparticles in aqueous extract of Hibiscus sabdariffa with enhanced photocatalytic activities," *RSC Advances*, vol. 7, no. 40, pp. 25149–25159, 2017.

[2] B. E. ElSaied, A. M. Diab, A. A. Tayel, M. A. Alghuthaymi, and S. H. Moussa, "Potent antibacterial action of phycosynthesized selenium nanoparticles usingSpirulina platensisextract," *Green Processing and Synthesis*, vol. 10, no. 1, pp. 49–60, 2021.

[3] E. Cremonini, E. Zonaro, M. Donini et al., "Biogenic selenium nanoparticles: characterization, antimicrobial activity and effects on human dendritic cells and fibroblasts," *Microbial Biotechnology*, vol. 9, no. 6, pp. 758–771, 2016.

[4] S. Menon, H. Agarwal, S. Rajeshkumar, P. J. Rosy, and V. K. Shanmugam, "Investigating the antimicrobial activities of the biosynthesized selenium nanoparticles and its statistical analysis," *Bionanoscience*, vol. 10, no. 1, pp. 122–135, 2020.

[5] F. Martínez-Esquivias, J. M. Guzmán-Flores, A. Pérez-Larios, N. González Silva, and J. S. Becerra-Ruiz, "A review of the antimicrobial activity of selenium nanoparticles," *Journal of Nanoscience and Nanotechnology*, vol. 21, no. 11, pp. 5383–5398, 2021.

[6] P. Korde, S. Ghotekar, T. Pagar, S. Pansambal, R. Oza, and D. Mane, "Plant extract assisted eco-benevolent synthesis of selenium nanoparticles-a review on plant parts involved, characterization and their recent applications," *Journal of Chemical Reviews*, vol. 2, no. 3, pp. 157–168, 2020.

[7] M. Ikram, B. Javed, N. I. Raja, and Z. U. R. Mashwani, "Biomedical potential of plant-based selenium nanoparticles: a comprehensive review on therapeutic and mechanistic aspects," *International Journal of Nanomedicine*, vol. 16, pp. 249–268, 2021.

[8] P. V. Baptista, M. P. McCusker, A. Carvalho et al., "Nano-strategies to fight multidrug resistant bacteria a battle of the titans," *Frontiers in Microbiology*, vol. 9, p. 1441, 2018.

[9] R. Vivas, A. A. T. Barbosa, S. S. Dolabela, and S. Jain, "Multidrug-resistant bacteria and alternative methods to control them: an overview," *Microbial Drug Resistance*, vol. 25, no. 6, pp. 890–908, 2019.

[10] F. Hashempour-Baltork, H. Hosseini, S. Shojaee-Aliabadi, M. Torbati, A. M. Alizadeh, and M. Alizadeh, "Drug resistance and the prevention strategies in food borne bacteria: an update review," *Advanced Pharmaceutical Bulletin*, vol. 9, no. 3, pp. 335–347, 2019.

[11] R. Lima, F. S. Del Fiol, and V. M. Balcão, "Prospects for the use of new technologies to combat multidrug-resistant bacteria," *Frontiers in Pharmacology*, vol. 10, p. 692, 2019.

[12] L. Marinescu, D. Ficai, O. Oprea et al., "Optimized synthesis approaches of metal nanoparticles with antimicrobial

applications," *Journal of Nanomaterials*, vol. 2020, Article ID 6651207, 14 pages, 2020.

[13] C. A. Soto-Robles, P. A. Luque, C. M. Gómez-Gutiérrez et al., "Study on the effect of the concentration of _Hibiscus sabdariffa_ extract on the green synthesis of ZnO nanoparticles," *Results in Physics*, vol. 15, article 102807, 2019.

[14] N. Thovhogi, A. Diallo, A. Gurib-Fakim, and M. Maaza, "Nanoparticles green synthesis by _Hibiscus sabdariffa_ flower extract: main physical properties," *Journal of Alloys and Compounds*, vol. 647, pp. 392–396, 2015.

[15] M. M. Abo Elsoud and E. M. El Kady, "Current trends in fungal biosynthesis of chitin and chitosan," *Bulletin of the National Research Centre*, vol. 43, no. 1, p. 59, 2019.

[16] A. A. Tayel, S. Moussa, K. Opwis, D. Knittel, E. Schollmeyer, and A. Nickisch- Hartfiel, "Inhibition of microbial pathogens by fungal chitosan," *International Journal of Biological Macromolecules*, vol. 47, no. 1, pp. 10–14, 2010.

[17] S. H. Moussa, A. A. Tayel, and A. I. Al-Turki, "Evaluation of fungal chitosan as a biocontrol and antibacterial agent using fluorescence-labeling," *International Journal of Biological Macromolecules*, vol. 54, pp. 204–208, 2013.

[18] A. A. Tayel, S. A. Ibrahim, M. A. Al-Saman, and S. H. Moussa, "Production of fungal chitosan from date wastes and its application as a biopreservative for minced meat," *International Journal of Biological Macromolecules*, vol. 69, pp. 471–475, 2014.

[19] M. S. Al-Saggaf, A. A. Tayel, M. A. Alghuthaymi, and S. H. Moussa, "Synergistic antimicrobial action of phycosynthesized silver nanoparticles and nano-fungal chitosan composites against drug resistant bacterial pathogens," *Biotechnology & Biotechnological Equipment*, vol. 34, no. 1, pp. 631–639, 2020.

[20] M. S. Al-saggaf, "Formulation of insect chitosan stabilized silver nanoparticles with propolis extract as potent antimicrobial and wound healing composites," *International Journal of Polymer Science*, vol. 2021, Article ID 5578032, 9 pages, 2021.

[21] M. S. Alsaggaf, S. H. Moussa, and A. A. Tayel, "Application of fungal chitosan incorporated with pomegranate peel extract as edible coating for microbiological, chemical and sensorial quality enhancement of Nile tilapia fillets," *International Journal of Biological Macromolecules*, vol. 99, pp. 499–505, 2017.

[22] A. A. Tayel, A. F. Elzahy, S. H. Moussa, M. S. Al-Saggaf, and A. M. Diab, "Biopreservation of shrimps using composed edible coatings from chitosan nanoparticles and cloves extract," *Journal of Food Quality*, vol. 2020, Article ID 8878452, 10 pages, 2020.

[23] A. Rangrazi, H. Bagheri, K. Ghazvini, A. Boruziniat, and M. Darroudi, "Synthesis and antibacterial activity of colloidal selenium nanoparticles in chitosan solution: a new antibacterial agent," *Materials Research Express*, vol. 6, no. 12, p. 1250h3, 2019.

[24] I. O. Oladele, T. F. Omotosho, and A. A. Adediran, "Polymer-based composites: an indispensable material for present and future applications," *International Journal of Polymer Science*, vol. 2020, Article ID 8834518, 12 pages, 2020.

[25] A. A. Tayel, W. F. El-Tras, and N. M. Elguindy, "The potentiality of cross-linked fungal chitosan to control water contamination through bioactive filtration," *International Journal of Biological Macromolecules*, vol. 88, pp. 59–65, 2016.

[26] M. S. Alsaggaf, S. H. Moussa, N. M. Elguindy, and A. A. Tayel, "Fungal chitosan and _Lycium barbarum_ extract as anti-_Listeria_ and quality preservatives in minced catfish," *International Journal of Biological Macromolecules*, vol. 104, pp. 854–861, 2017.

[27] S. Alsharari, A. A. Tayel, and S. H. Moussa, "Soil emendation with nano-fungal chitosan for heavy metals biosorption," *International Journal of Biological Macromolecules*, vol. 118, pp. 2265–2268, 2018.

[28] A. I. Alalawy, H. A. El Rabey, F. M. Almutairi et al., "Effectual anticancer potentiality of loaded bee venom onto fungal chitosan nanoparticles," *International Journal of Polymer Science*, vol. 2020, Article ID 2785304, 9 pages, 2020.

[29] H. A. El Rabey, F. M. Almutairi, A. I. Alalawy et al., "Augmented control of drug-resistant _Candida_ spp. via fluconazole loading into fungal chitosan nanoparticles," *International Journal of Biological Macromolecules*, vol. 141, pp. 511–516, 2019.

[30] M. Alghuthaymi, A. Diab, A. Elzahy, K. Mazrou, A. A. Tayel, and S. H. Moussa, "Green biosynthesized selenium nanoparticles by cinnamon extract and their antimicrobial activity and application as edible coatings with nano-chitosan," *Journal of Food Quality*, vol. 2021, Article ID 6670709, 10 pages, 2021.

[31] M. S. Al-Saggaf, A. A. Tayel, M. O. Ghobashy, M. A. Alotaibi, M. A. Alghuthaymi, and S. H. Moussa, "Phytosynthesis of selenium nanoparticles using the costus extract for bactericidal application against foodborne pathogens," *Green Processing and Synthesis*, vol. 9, no. 1, pp. 477–487, 2020.

[32] Y. Choong, N. S. A. Yousof, M. I. Wasiman, J. A. Jamal, and Z. Ismail, "Determination of effects of sample processing on Hibiscus sabdariffa L. using tri-step infrared spectroscopy," *Journal of Analytical & Bioanalytical Techniques*, vol. 7, no. 5, pp. 1–9, 2016.

[33] S. Johson, S. A. Razack, P. Sellaperumal et al., "Green synthesis of iron oxide nanoparticles using Hibiscus rosa-sinensis for fortifying wheat biscuits," *EC Microbiology*, vol. 2, no. 5, pp. 1–9, 2020.

[34] C. M. Paraíso, S. S. dos Santos, C. Y. L. Ogawa, F. Sato, O. A. dos Santos, and G. S. Madrona, "Hibiscus sabdariffa L. extract: characterization (FTIR-ATR), storage stability and food application," *Emirates Journal of Food and Agriculture*, vol. 2020, pp. 55–61, 2020.

[35] D. Gingasu, I. Mindru, L. Patron et al., "Green synthesis methods of $CoFe_2O_4$ and Ag-$CoFe_2O_4$ nanoparticles using hibiscus extracts and their antimicrobial potential," *Journal of Nanomaterials*, vol. 2016, Article ID 2106756, 12 pages, 2016.

[36] N. Srivastava and M. Mukhopadhyay, "Biosynthesis and structural characterization of selenium nanoparticles Using Gliocladium roseum," *Powder Technology*, vol. 26, no. 5, pp. 1473–1482, 2015.

[37] Y. Chen and H. Ming, "Review of surface plasmon resonance and localized surface plasmon resonance sensor," *Photonic Sensors*, vol. 2, no. 1, pp. 37–49, 2012.

[38] V. Ganesan, "Biogenic synthesis and characterization of selenium nanoparticles using the flower of Bougainvillea spectabilis Willd," *International Journal of Science and Research*, vol. 4, pp. 690–695, 2015.

[39] W. Chen, L. Yue, Q. Jiang, X. Liu, and W. Xia, "Synthesis of varisized chitosan-selenium nanocomposites through heating treatment and evaluation of their antioxidant properties," *International Journal of Biological Macromolecules*, vol. 114, pp. 751–758, 2018.

[40] S. Bhattacharjee, "DLS and zeta potential - what they are and what they are not," *Journal of Controlled Release*, vol. 235, pp. 337–351, 2016.

[41] L. Rao, Y. Ma, M. Zhuang, T. Luo, Y. Wang, and A. Hong, "Chitosan-decorated selenium nanoparticles as protein carriers to improve the in vivo half-life of the peptide therapeutic BAY 55-9837 for type 2 diabetes mellitus," *International Journal of Nanomedicine*, vol. 9, pp. 4819–4828, 2014.

[42] L. A. Portillo-Torres, A. Bernardino-Nicanor, J. Mercado-Monroy et al., "Antimicrobial Effects of Aqueous Extract from Calyces of *Hibiscus sabdariffa* in CD-1 Mice Infected with Multidrug-Resistant Enterohemorrhagic *Escherichia coli* and *Salmonella* Typhimurium," *Journal of Medicinal Food*, 2021.

[43] E. Jung, Y. Kim, and N. Joo, "Physicochemical properties and antimicrobial activity of Roselle Hibiscus sabdariffa L," *Journal of the Science of Food and Agriculture*, vol. 93, no. 15, pp. 3769–3776, 2013.

[44] I. Alshami and A. E. Alharbi, "Antimicrobial activity of Hibiscus sabdariffa extract against uropathogenic strains isolated from recurrent urinary tract infections," *Asian Pacific Journal of Tropical Disease*, vol. 4, no. 4, pp. 317–322, 2014.

[45] S. Abdel-Shafi, A. R. Al-Mohammadi, M. Sitohy et al., "Antimicrobial activity and chemical constitution of the crude, phenolic-rich extracts of Hibiscus sabdariffa, Brassica oleracea and Beta vulgaris," *Molecules*, vol. 24, no. 23, p. 4280, 2019.

[46] A. H. Zyoud, F. Saleh, M. H. Helal, R. Shawahna, and H. S. Hilal, "Anthocyanin-sensitized TiO_2 nanoparticles for phenazopyridine photodegradation under solar simulated light," *Journal of Nanomaterials*, vol. 2018, Article ID 2789616, 14 pages, 2018.

[47] G. Zhao, X. Wu, P. Chen, L. Zhang, C. S. Yang, and J. Zhang, "Selenium nanoparticles are more efficient than sodium selenite in producing reactive oxygen species and hyper-accumulation of selenium nanoparticles in cancer cells generates potent therapeutic effects," *Free Radical Biology and Medicine*, vol. 126, pp. 55–66, 2018.

[48] D. Chudobova, K. Cihalova, S. Dostalova et al., "Comparison of the effects of silver phosphate and selenium nanoparticles on Staphylococcus aureus growth reveals potential for selenium particles to prevent infection," *FEMS Microbiology Letters*, vol. 351, no. 2, pp. 195–201, 2014.

[49] A. A. Tayel, S. H. Moussa, W. F. El-Tras, N. M. Elguindy, and K. Opwis, "Antimicrobial textile treated with chitosan from _Aspergillus niger_ mycelial waste," *International Journal of Biological Macromolecules*, vol. 49, no. 2, pp. 241–245, 2011.

[50] X. D. Shi, Y. Q. Tian, J. L. Wu, and S. Y. Wang, "Synthesis, characterization, and biological activity of selenium nanoparticles conjugated with polysaccharides," *Critical Reviews in Food Science and Nutrition*, vol. 61, no. 13, pp. 2225–2236, 2021.

[51] A. M. Abdelghany, A. A. Menazea, and A. M. Ismail, "Synthesis, characterization and antimicrobial activity of Chitosan/Polyvinyl Alcohol blend doped with Hibiscus Sabdariffa L. extract," *Journal of Molecular Structure*, vol. 1197, pp. 603–609, 2019.